MAGNETIC
RESONANCE
IMAGING

ELSEVIER

Simultaneous observations of haemolymph flow and ventilation in marine spider crabs at different temperatures: a flow weighted MRI study

Christian Bock*, Markus Frederich†, Rolf-M. Wittig, Hans-O. Pörtner

Alfred-Wegener-Institute for Polar and Marine Research, Columbusstraße, 27568 Bremerhaven, Germany

Abstract

In vivo magnetic resonance imaging (MRI) and angiography were applied to the marine spider crab *Maja squinado* for a study of temperature effects and thermal tolerance. Ventilation and haemolymph circulation were investigated during progressive cooling from 12°C to 2°C. The anatomical resolution of MR images from *Maja squinado* obtained with a standard spin echo sequence were suitable to resolve the structures of various internal organs. The heart of the animal could be depicted without movement artifacts. The use of a flow compensated gradient echo sequence allowed simultaneous observations of ventilation, reflected by water flow through the gill chambers as well as of haemolymph flow. Simultaneous investigation of various arteries was possible by use of flow weighted MRI. In addition to those accessible by standard invasive flow sensitive doppler sensors, flow changes in gill, leg arteries and the venous return could be observed. Both ventilation and haemolymph flow decreased during progressive cooling and changes in haemolymph flow varied between arteries. Haemolymph flow through the Arteria sternalis, some gill and leg arteries was maintained at low temperatures indicating a reduced thermal sensitivity of flow in selected vessels. In support of previous invasive studies of haemolymph flow as well as heart and ventilation rates, the results demonstrate that the operation of gills and the maintenance of locomotor activity are critical for cold tolerance. A shift in haemolymph flow between arteries likely occurs to ensure the functioning of locomotion and ventilation in the cold. © 2001 Elsevier Science Inc. All rights reserved.

1. Introduction

Recently, *in vivo* NMR spectroscopy has become a useful tool for physiological studies of aquatic organisms (for review see [1,2]). Compared to freshwater animals the application of NMR techniques to marine organisms is complicated by the electrical properties of seawater, where the high ion content causes inductive loss of signal intensity [3]. Therefore, most of the reported NMR studies are spectroscopy studies performed on perfused organs or small marine animals [4–7]. In only a few cases MR imaging techniques were applied to marine organisms *in vivo* [8–11]. In these studies MR imaging was used to depict the anatomy of marine animals with different MR contrast parameters (in particular, T_1 and T_2 weighted MRI).

Aim of the present study was to develop an experimental set-up to study ventilation and haemolymph flow of the marine spider crab *Maja squinado* (Herbst) in response to falling temperatures. Gradient echo MRI sequences with flow compensation were applied. This approach has frequently been used for MR angiography in medical research. In addition, these techniques allow to visualize the ventilation of aquatic animals [12,13]. Therefore, using MRI, it should be possible to observe ventilation and blood flow at the same time.

Pörtner et al. led to the hypothesis that thermal tolerance is limited by insufficient oxygen supply to tissues at extreme temperatures [14,15]. This implies that not only oxygen uptake through the gills, but also maintenance of ventilation and of circulation is critical for thermal tolerance [16]. Furthermore, Frederich et al. [17] have shown that during progressive cooling the change in haemolymph flow in the

* Corresponding author. Tel.: +49-471-4831-1380; fax: +49-471-4831-1149.

E-mail address: cbock@awi-bremerhaven.de (C. Bock).

† Present address: Brigham and Women's Hospital (Harvard Medical School), Boston, MA 02115, USA.

marine spider crab *Maja squinado* varied between arteries. For a more complete view of the whole circulatory system in *Maja squinado*, we investigated ventilation as well as haemolymph flow during progressive cooling from 12°C to 2°C with multi slice flow weighted MRI. These results were compared with ultrasonic doppler flow measurements of different arteries as well as analyses of ventilation rates at different temperatures [17].

Like all brachyuran crustaceans *Maja squinado* possesses an open circulatory system consisting of a single chambered dorsal heart in the cardial sinus, various well-developed arteries but no venous vessels. Haemolymph leaving the heart cranially is supplied to the brain via a single Arteria anterior and to the stomach region via two Arteriae lateralis. Two Arteriae hepaticae originating in the center of the heart lead into the hepatopancreas. The largest artery originating at the caudal end of the heart is the Arteria sternalis. This vessel runs to the ventral side of the animal with a bifurcation to the abdomen (Arteria ventralis abdominalis) and then turns in cranial direction with ramifications to each walking leg and to cephalic appendages. Venous return is led through lacunes into the pericardial sinus where it reenters the heart [18]. Despite this open circulatory system, crabs are able to regulate haemolymph flow through the arteries as well as through the lacunes by changing peripheral resistance [19–21].

2. Materials and methods

Crabs ($n = 5$, carapace diameter ca. 13 cm, weight 450–650 g) were purchased from local fishermen in Roscoff, France, 1998 and kept in aerated recirculating seawater aquaria at 12°C. For MR experiments animals were immobilized in a peripex perfusion chamber (19.4 cm diameter, 40 cm length) by fixation of a T-shaped bar (height 2.5 cm, width 1 cm) to the dorsal carapace by use of dental wax (Fig. 1a). This allowed the animals to move their legs and piles, while only the central body was fixed to prevent movement artifacts in the MR images. Seawater was supplied to the experimental set-up by hydrostatic pressure as depicted in Bock et al. [11] (Fig. 1b).

Temperature was measured inside the chamber via optical fibers using a fluoroptic thermometer (Luxtron 504, Polytec, Waldheim, Germany). Temperature data were sampled continuously (sampling rate 10/min) and stored on a computer (MacLab system, AD Instruments, Australia). Temperature control was achieved by a cryostat connected to the upper water reservoir. Animals were allowed to acclimate to 12°C for about 12 h inside the magnet before starting experimentation. Temperature was reduced from 12°C to 2°C within 8 h and returned to control conditions after finishing the imaging studies. Sets of MR images were recorded once every hour over a maximum period of 30 min.

All MR experiments were carried out with a Bruker Biospec 4.7 T DBX system with actively shielded gradient coils (50 mT/m). A ^{1}H cylindrical resonator (20 cm diameter) adapted for high conductivity samples was used for signal excitation and reception. After optimization of the chamber position via scout images in all three directions, flow compensated gradient echo images [22] were sampled in coronal and axial directions. Parameters were as follows: matrix size: 256 × 192, TR: 100 ms, TE: 10 ms, FOV: 12 cm, 4 to 6 slices (slice thickness 2.2 mm, 4 averages) and a flip angle of 80° (using a 4000 μs hermite pulse) resulting in a scan time of 2.5 min to 3.8 min. In some cases additional multi slice flow weighted MR images (30 slices) were collected at 12°C and at 5°C (measuring time 20 min). Water flow through the system was reduced during data acquisition to minimize signal intensity originating from seawater flow surrounding the animal. Three-dimensional maximum intensity maps (MIPs) and surface projection maps were postprocessed from multi slice data sets with a 3D graphic routine (Xtip, ParaVision, Bruker, Ettlingen, Germany).

For anatomical studies multi slice RARE images [23] were collected in coronal direction (matrix: 256 × 192, FOV = 12 cm, 10 slices with a slice thickness of 2 mm, slice distance 2.5 mm, TR = 3000 ms, TE = 18.4 ms, 8 averages, rare factor 16, scan time 10 min 32 s).

2.1. Data analysis and statistics

The contrast in flow compensated gradient echo MRI sequences depends on different parameters such as T_1, T_2, magnetic field inhomogeneities (T_2^*) and flow. Mean signal intensity was determined from regions of interest (ROI) in different arteries and the gill chambers compared to regions of interest where flow effects could be excluded (e.g., carapace and air). The latter ROIs are considered as noise. For qualitative comparisons of flow, the ratio of ROIs and noise were calculated to compensate for potential T_1, T_2, and T_2^* contrast changes. Previously performed ultrasonic doppler measurements [17] have shown that almost no haemolymph circulated in the hepatic and the lateral arteries at low temperatures. In support of these findings, the S/N ratio of the ROIs from the hepatic artery in coronal images and the lateral arteries in transversal images displayed no obvious flow contributions at low temperatures, as confirmed by comparing the signal intensity contrast between vessels and tissue in the MR images (e.g., Fig. 5D). Therefore, the lowest S/N ratios of these arteries were subtracted from the different S/N ratios of the individual animals and considered as a threshold for image contrast with no flow contribution in the coronal images (normalized from hepatic S/N ratio) and transversal images (normalized from lateral S/N ratio). Ventilation changes were determined by subtracting the lowest S/N ratio from an ROI in the gill chamber. Normalized S/N ratios from ROIs above these levels were considered to indicate haemolymph flow. Results are given as means ± standard deviation.
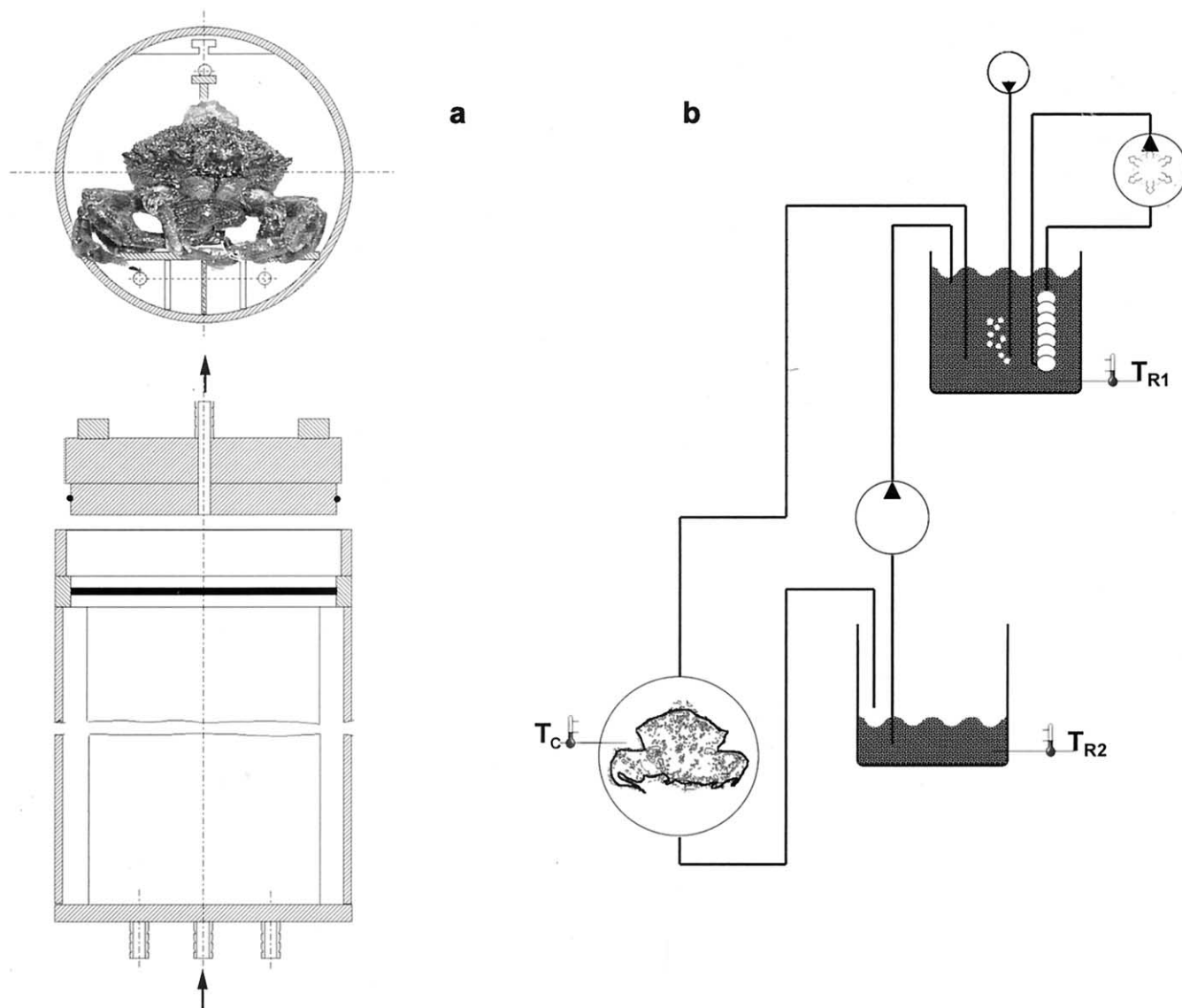
Fig. 1. (a) Flow-through chamber (19.4 cm diameter, 40 cm length) constructed for *in vivo* NMR measurements in crustaceans (max. diameter 15 cm). The animals were fixed with dental wax on a T-shaped bar and positioned relative to the resonator inside the chamber. Indicated are the water inflow and outflow passages (see arrows). (b) Experimental set-up. A constant flow of seawater (up to 1.5 l/min) was supplied by hydrostatic pressure. Seawater (approx. 50 l) was bubbled with air in the header tank, temperature was measured in the chamber (T_C) using a fluoroptic thermometer connected to a MacLab system. Temperature control was achieved by a cryostat connected to the upper water reservoir.

An exponential trend was fitted to the S/N changes of the different curves and Q_{10} values of flow changes were calculated according to:

$$Q_{10} = \left(\frac{S_{T2}}{S_{T1}}\right)^{10/(T2-T1)}$$

S is the flow calculated from exponential fits at T2 = 12°C and T1 = 1°C.

3. Results

MR experiments on *Maja squinado* were carried out for several days without any obvious harmful effects on the animals (data not shown). Intensive movements of the legs of the animals could be observed only directly after placing the animals inside the magnet. MR scanner noise had no obvious effect on the behaviour or movement of the animals.

Fig. 2 presents a set of coronal multi slice RARE images for anatomical studies through the carapace of *Maja squinado*. The quality of the MR images is suitable to identify internal structures of different organs, despite the disturbing high conductivity of the surrounding seawater. Susceptibility artifacts from carapace-tissue transitions and remaining air in the gill chambers were very small (see bright spots in Fig. 2D). The musculature of the legs (a), the hepatopancreas and the gonadal tissue (b) as well as the gills (c) could
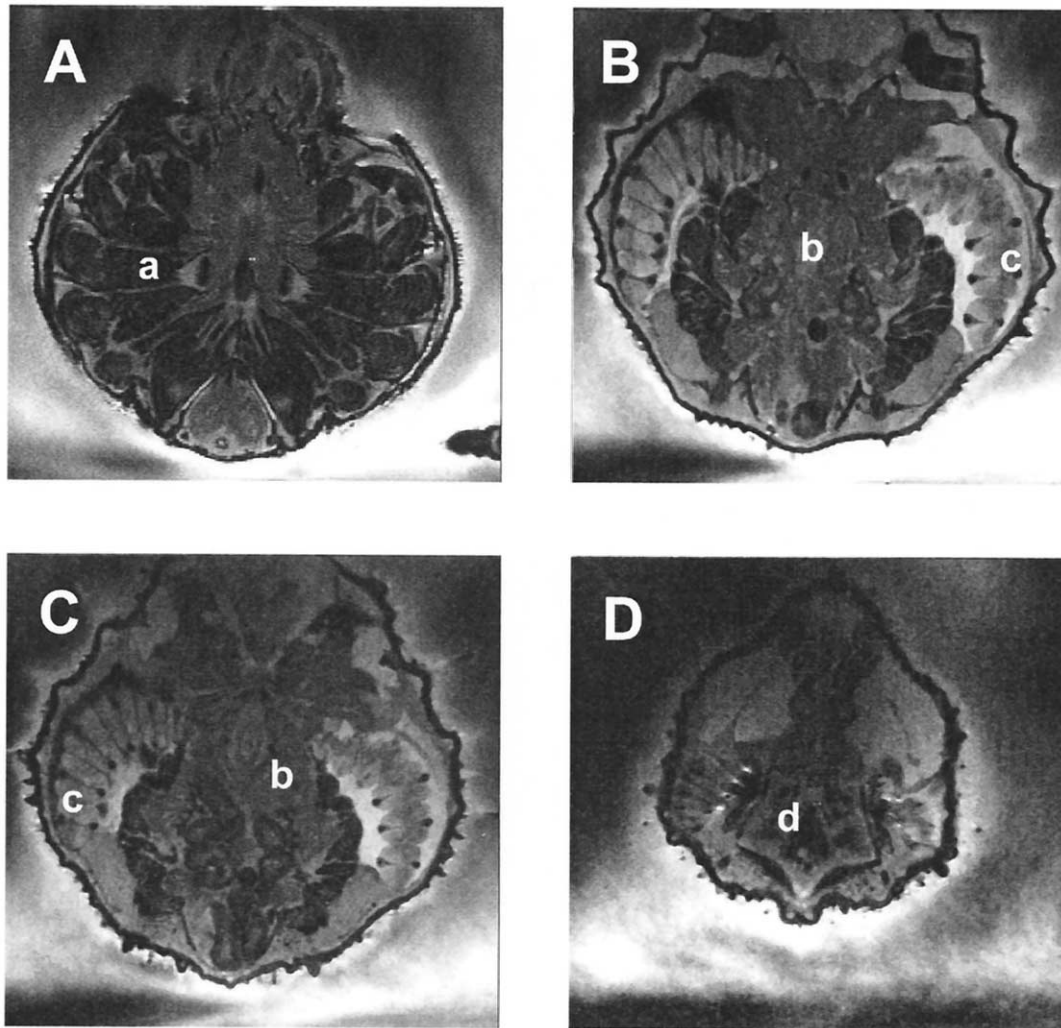
Fig. 2. Coronal multi slice anatomical images of the body of the marine spider crab *Maja squinado* under control conditions ($T = 12°C$) (see Materials and methods for imaging parameters). Anterior at top of images. Layers extended from the leg musculature (A) to the upper back (D). Excellent distinction of individual organs was possible in the images (a: leg muscle, b: hepatopancreas and gonadal tissue, c: gills, d: heart), despite of high inductive loss elicited by the surrounding seawater and despite the inhomogeneity inside the animal (see bright spots due to residual air inside the gill chambers in Fig. 2D).

be resolved. Furthermore, the heart could be observed without movement artifacts (d).

Fig. 3 shows the same set of images collected with multi slice flow weighted MR imaging. Haemolymph flow could be detected in the surroundings of the leg musculature (a), the Arteria ventralis abdominalis (b), through the Arteria sternalis (c), the arteries of the gills (d), as well as in the heart and the pericardial sinus (i). Furthermore, venous return through lacunes (e) as well as flow through the Arteriae hepaticae in the hepatopancreas (f), through the Arteriae lateralis supplying haemolymph to the stomach region (g) and the Arteria anterior (h) could be resolved. A more diffuse signal arose from water flowing through the gill chambers reflecting the ventilatory activity of the animal (k).

Three dimensional maximum intensity projection maps (MIPs) post-processed from multi slice flow weighted images are presented in Fig. 4. The MIPs of two animals under control conditions ($T = 12°C$) are shown, where the cranial end of the animals is located at the top of the images. The view through the MIPs is from ventral through the body to the dorsal side. Ventilatory water currents generated by the scaphognathites are represented by the diffuse signal reaching from the scaphognathites in the mouth region out of the gill chambers (see arrows). The pearl chain like structures of the arteries results from the slice thickness of 2.2 mm and the hermite pulses. The animal in Fig. 4B ventilated the left gill chamber only and haemolymph flow through the right gill arteries was reduced in comparison to the left gill arteries. The ventilation of one gill chamber only, is a common observation in decapod crustaceans [24].

Coronal flow weighted MR images of *Maja squinado* collected at different temperatures are presented in Fig. 5. No artifacts induced by body movements could be observed and the position of the image slice did not change over the whole experimental period of 8 h, indicating sufficient fix-
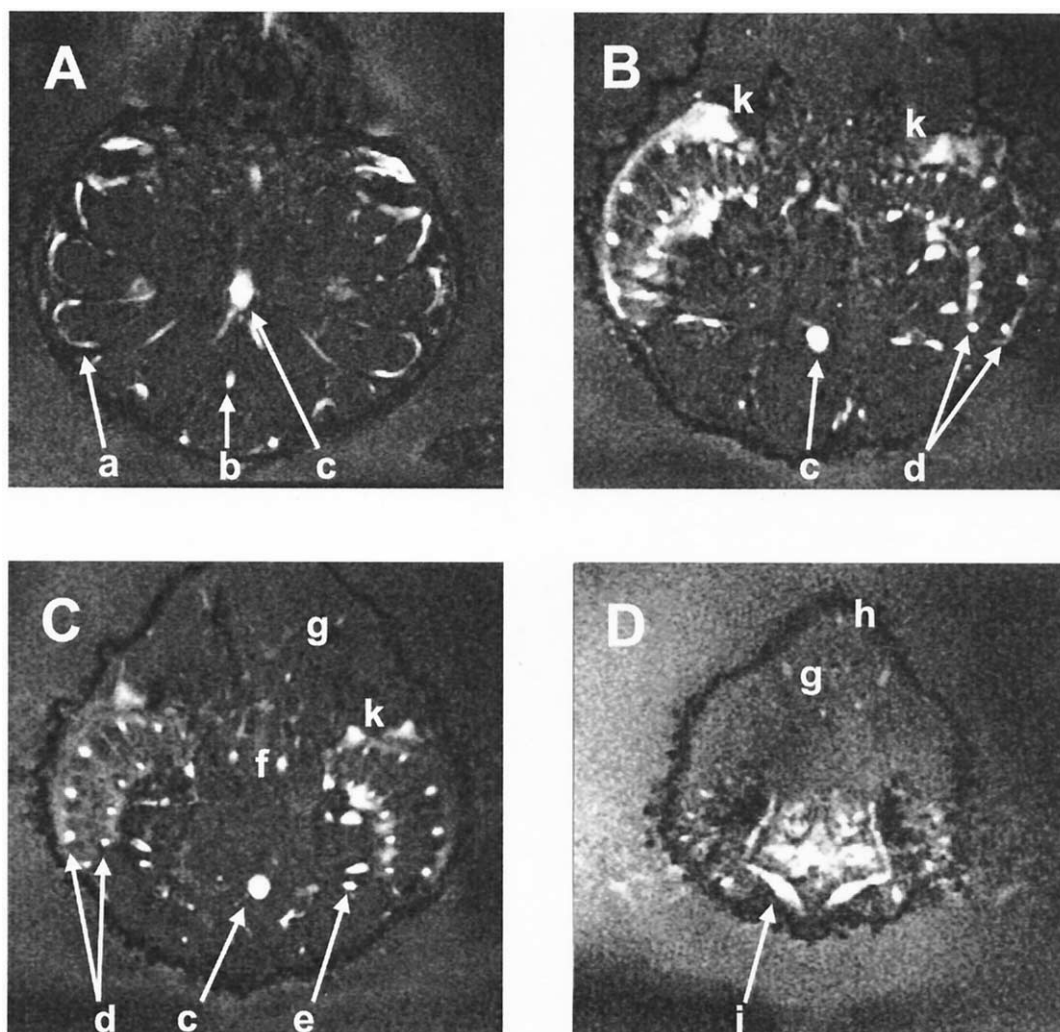
Fig. 3. Flow weighted MR images from the set of slices depicted in Fig. 2 (imaging parameters see text). Haemolymph flow can be detected surrounding the leg muscles (a), in the Arteria ventralis abdominalis (b), in the Arteria sternalis (c), in the ascending and descending gill arteries (d), in lacunes (venous return, e), in the two Arteriae hepaticae of the hepatopancreas (f), in the two Arteriae lateralis supplying haemolymph to the stomach (g), in the Arteria anterior (h), and inside the heart with its pericardial sinus (i). The diffuse signal intensity in the gill chambers resulted from ventilatory activity (k).

ation of the carapace. Nevertheless, changes in the signal intensity of water layers surrounding the animal could be observed in some images due to leg movements and ventilation (data not shown). The highest signal arose from gill arteries (a), the Arteria sternalis (b), venous return (c), and the hepatic arteries (d). Again, the bright and diffuse signal of water flowing through the gill chambers could be observed (e) as well as the Arteria ventralis abdominalis (f), the Arteriae lateralis (g), the Arteria anterior (h), and one leg artery (i). Cooling induced a decrease in signal intensity reflecting a decrease in haemolymph flow with temperature. Below 6°C ventilation was largely reduced confirmed by the vanishing signal of water flow inside the gill chambers (B + C). At low temperatures almost all signals arising from arterial as well as venous return disappeared. Return to control temperatures resulted in an increase in haemolymph flow in all arteries and a rise in water flow in gill chambers

(data not shown). Only one out of 5 animals did not recover from the cooling protocol.

Fig. 6 presents three dimensional surface projection maps obtained from multi slice flow weighted images at 11°C (A) and at 5°C (B). The animal's dorsal side is pointing to the top of the figure and the cranial end to the right. Haemolymph flow in the heart, the gill arteries, the Arteria sternalis, the hepatic arteries, some arteries of the legs and ventilatory flow through the left gill chamber is represented in the surface projection map. Haemolymph flow was reduced at lower temperatures inside the heart and in the hepatic arteries (arrow, Fig. 6A) visible in the surface projection map at 5°C. In contrast, flow through some gill arteries and the Arteria sternalis was maintained reflecting a shift in haemolymph flow between vessels (Fig. 6B).

The changes in haemolymph flow in the Arteria sternalis and in ventilatory flow as obtained from MR imaging data
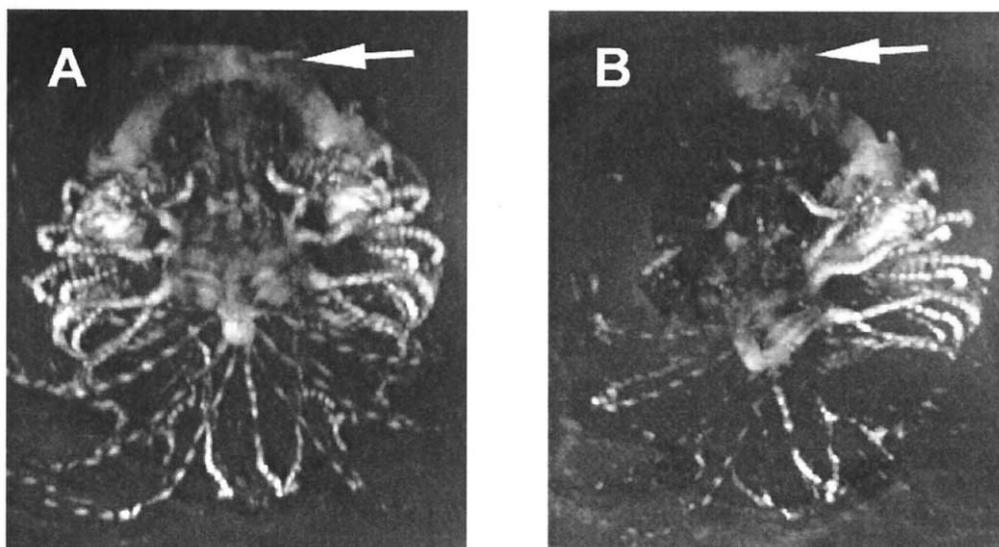
Fig. 4. Examples of three dimensional maximum intensity projection maps (MIPs) from two animals under control conditions. The view through the MIPs is from ventral through the body to the dorsal side (animals anterior at top of image). Ventilation could be detected by the diffuse water flow generated by the scaphognathites (see arrows) into and out of the gill chambers. The animal in Fig. 4B ventilated only the left gill chamber (visible to the right of the figure), haemolymph flow through the right gill arteries was reduced at the same time.

are compared to the respective data obtained from ultrasonic pulsed doppler flow measurements and photoplethysmography [16,17] in Fig. 7. The patterns of changes in haemolymph flow as well as in ventilation rates are in good qualitative agreement between the different methods with a complete collapse in ventilation in the cold ($Q_{10} = 25.5$) and an almost 4-fold reduction in haemolymph flow through the Arteria sternalis between 12°C and 1°C ($Q_{10} = 4.2$), as determined from the exponential approximation.

Fig. 8 depicts flow changes in various haemolymph vessels. Flow rates decreased at lower temperatures, but rates remained highest in Arteria sternalis (see Fig. 7A), gill ($Q_{10} = 2.3$) and leg arteries ($Q_{10} = 1.8$) at all temperatures. In contrast, flow collapsed in hepatic ($Q_{10} = 7.7$) and the two lateral arteries ($Q_{10} = 19.1$ and 14.5) and was largely reduced in venous lacunes ($Q_{10} = 6.7$) in the cold. Haemolymph flow in the anterior artery was lowest under control conditions and decreased only slightly in the cold ($Q_{10} = 3.1$). Leg arteries could not be observed in every animal since legs sometimes were moved out of the field of view during the experiments.

4. Discussion

Aim of this study was the application of MR imaging techniques to a study of thermal effects on circulation and ventilation in a marine crustacean. The ion strength and high conductivity of seawater changes the electrical properties of HF-coils and leads to signal loss and line broadening [3]. We used a resonator especially adapted for high conductivity samples. Since the maximum HF-power was limited to 1 kW, it was not possible to use shorter and sharper pulses

like the sinc pulse with a typical pulse length of 1000 μs due to the high amount of seawater (the resonator was almost filled with seawater). Therefore, hermite pulses with 4000 μs length were used, which led to a slice thickness of 2 mm minimum. Increasing the number of averages and thus acquisition time did not cause any blurring effects or ghosting, because the animals remained in a resting position with an adequate fixation. The S/N ratio and the anatomical resolution were sufficient to visualize internal structures of different organs. Since the heart rate of these animals is relatively low (52.9 ± 14.8 min^{-1} at 12°C) [16], it was possible to image the heart free of artifacts. Moreover, RARE and gradient echo techniques are very sensitive to susceptibility effects and a good field and object homogeneity are crucial for a good image quality. To overcome inhomogeneity effects due to field changes between carapace, tissue and air, the animal chamber was filled completely with seawater, representing a homogeneous cylinder inside the probe, such that global shimming could be performed automatically. Indeed, the only susceptibility artifacts in the RARE images arose from air bubbles inside the gill chambers, Fig. 2D, which were sometimes introduced by handling of the animals at the beginning of the experiment.

The influence of cooling on haemolymph flow and on ventilation in *Maja squinado* was investigated using flow weighted MR imaging. Crabs possess an open circulatory system with a single chambered heart and well developed arteries, while veins are absent [18] (see above). Nonetheless, arteries as well as venous lacunes could be detected in flow weighted images with a reasonable time resolution that even allowed individual analysis of small arteries (Fig. 8). In previous studies water flowing through the gill chambers of fish [12] and through the egg masses of female Brachyu-
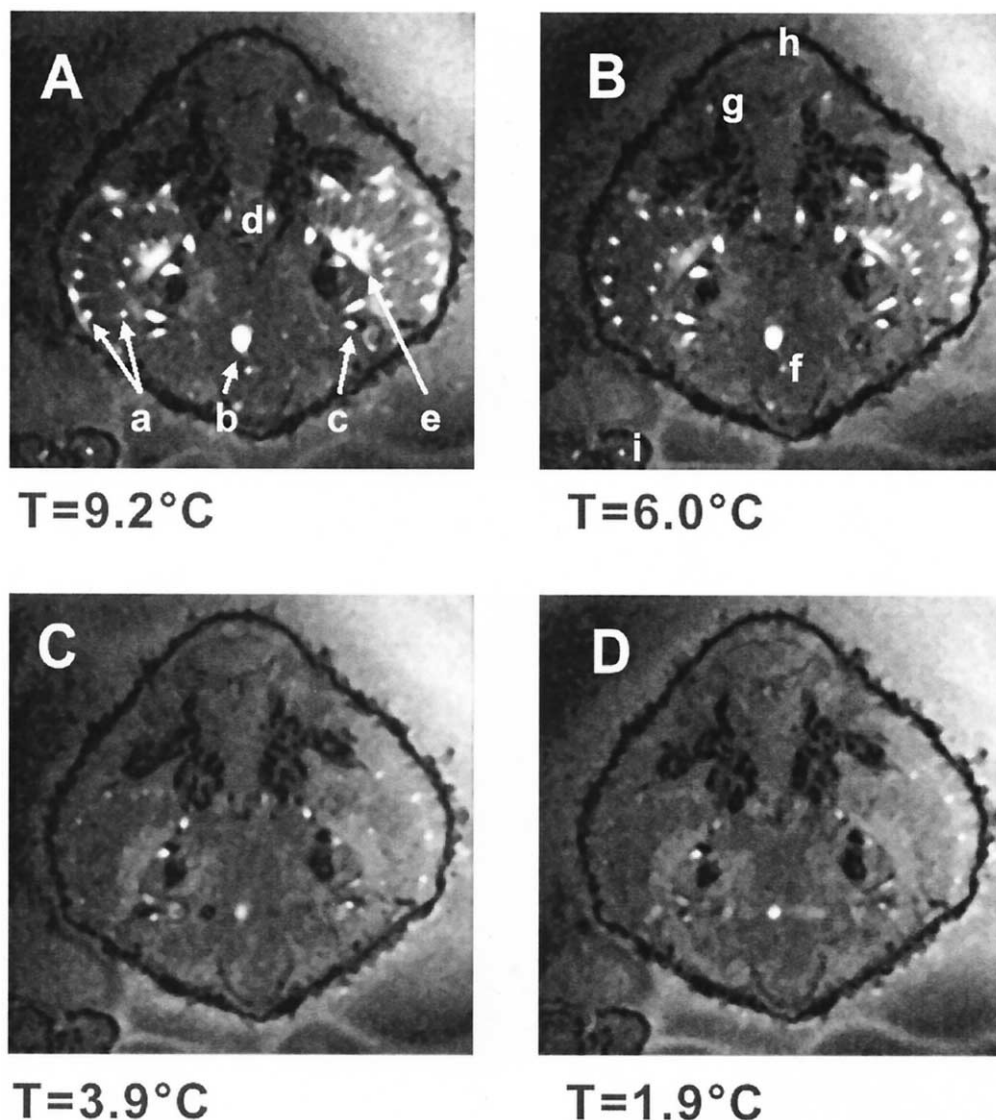
Fig. 5. Coronal flow weighted images of the spider crab *Maja squinado* at decreasing temperatures (from A to D, anterior at top of images). The arrows indicate: a) gill arteries, b) Arteria sternalis, c) venous return, hepatic arteries (d), ventilatory activity (e), Arteria ventralis abdominalis (f), Arteriae lateralis (g), the Arteria anterior (h), and one leg artery (i). Below 6°C ventilation dropped largely, indicated by the loss of diffuse intensity in the gill chambers (arrow e). Haemolymph flow through the arteries displayed the same pattern.

ran crabs [13] could be observed in MR images and attributed to the ventilatory activity of the animal. In the present study the maximum intensity maps under control conditions revealed that ventilatory and haemolymph flows are linked. Ventilatory activity and haemolymph flow in the gills were detected in one gill chamber only, whereas at the same time water flow and haemolymph flow through the gill arteries of the other chamber were reduced (Fig. 4B). It is well known that decapod crustaceans are able to regulate haemolymph distribution depending on factors like activity level, temperature, or PO_2 [16,19,20,24,25]. This study reveals that ventilation and gill blood flow under resting conditions are controlled in parallel.

During progressive cooling below 7°C ventilation was largely reduced and signal intensities in the Arteria sternalis decreased more or less in parallel (Fig. 5 + 7). In general, it appears that the reduction in ventilation as well as in haemolymph flow go hand in hand. However, the S/N ratios, obtained from a superposition of areas with and without flow, likely overestimated the actual flow especially at low temperatures and flow rates close to zero. Moreover, small deviations from optimum flip angles could induce big differences in tissue contrast. Accordingly, different tissues could be distinguished in the MRIs in Fig. 5 but not in Fig. 3, where signal intensity was similar for all tissues. Under low flow conditions fluctuating contrast parameters may exert an even larger effect. In Fig. 5D for example various tissues inside the carapace generated signal intensities much higher than the carapace or air, which were previously considered as noise. Accordingly, S/N ratios might over-
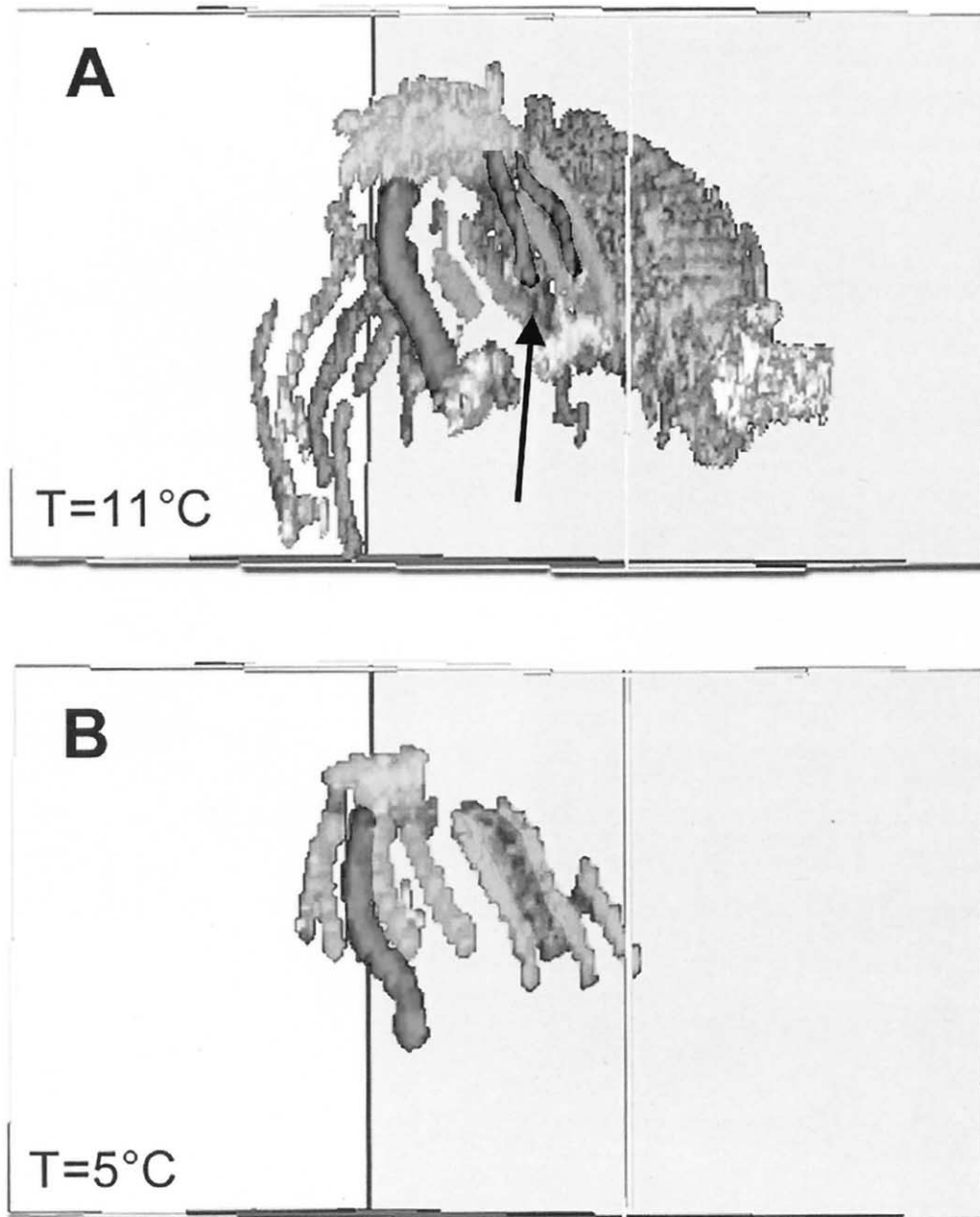
Fig. 6. Three dimensional surface projection maps obtained from flow weighted imaging data of *Maja squinado* at 11°C (A) and at 5°C (B). Haemolymph in the heart and through various vessels as well as ventilatory flow through the left gill chamber at 11°C become visible. At 5°C haemolymph flow was reduced and ventilation through the left gill chamber stopped. Nevertheless, haemolymph flow through some gill arteries and the Arteria sternalis was maintained, whereas the flow through the hepatic arteries (figure A, arrow) vanished.

indicate flow even when no obvious flow could be detected (e.g., hepatic arteries in Fig. 5D). Nonetheless, calculation of S/N ratios is essential to compensate for cooling induced changes in tissue contrast. To correct for the overestimation of S/N ratios, flow contrasts were normalized, setting the lowest S/N ratios obtained at low temperatures to zero for the hepatic artery in coronal images and for the lateral artery in transversal images (see Materials & methods).

With these corrections, the pattern of changes in ventilation rates and in haemolymph flow through the Arteria sternalis detected by the doppler technique and by photo-

plethysmography were in good qualitative agreement with the MR recordings of changes in ventilatory and haemolymph flows (Fig. 7). The exponential decay of haemolymph flow in the Aorta sternalis determined from the MR data confirmed the 4-fold reduction in haemolymph flow measured by the doppler technique (Fig. 7A + B), thus validating the normalization of the S/N ratios.

Fig. 8 summarizes the relative signal intensity changes determined from ROIs of some vessels from the flow weighted MR data. Ventilatory flow (Fig. 7) and haemolymph flow through the hepatic, anterior, and lateral arteries
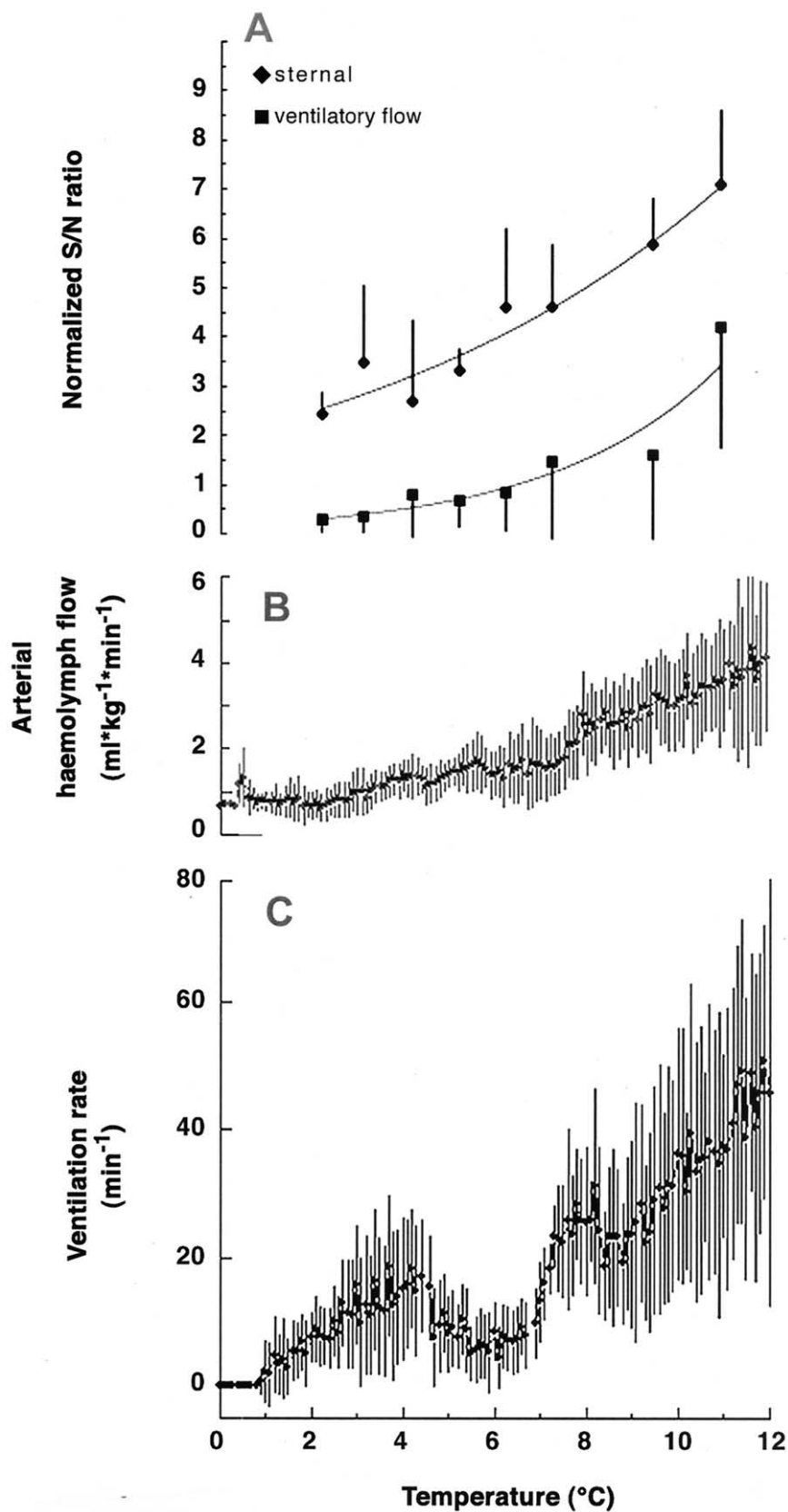
Fig. 7. Comparison of flow weighted imaging data collected from the Arteria sternalis ($n = 5$) and from water flow in gill chambers ($n = 5$) (A) with results obtained by ultrasonic doppler recordings of haemolymph flow (B) and by photoplethysmographic measurements of ventilation rate (C) during progressive cooling. The pattern of change in the MR data is in good qualitative agreement with the measurements of arterial haemolymph flow and ventilation rate. (B + C as adopted from ref. 16,17).
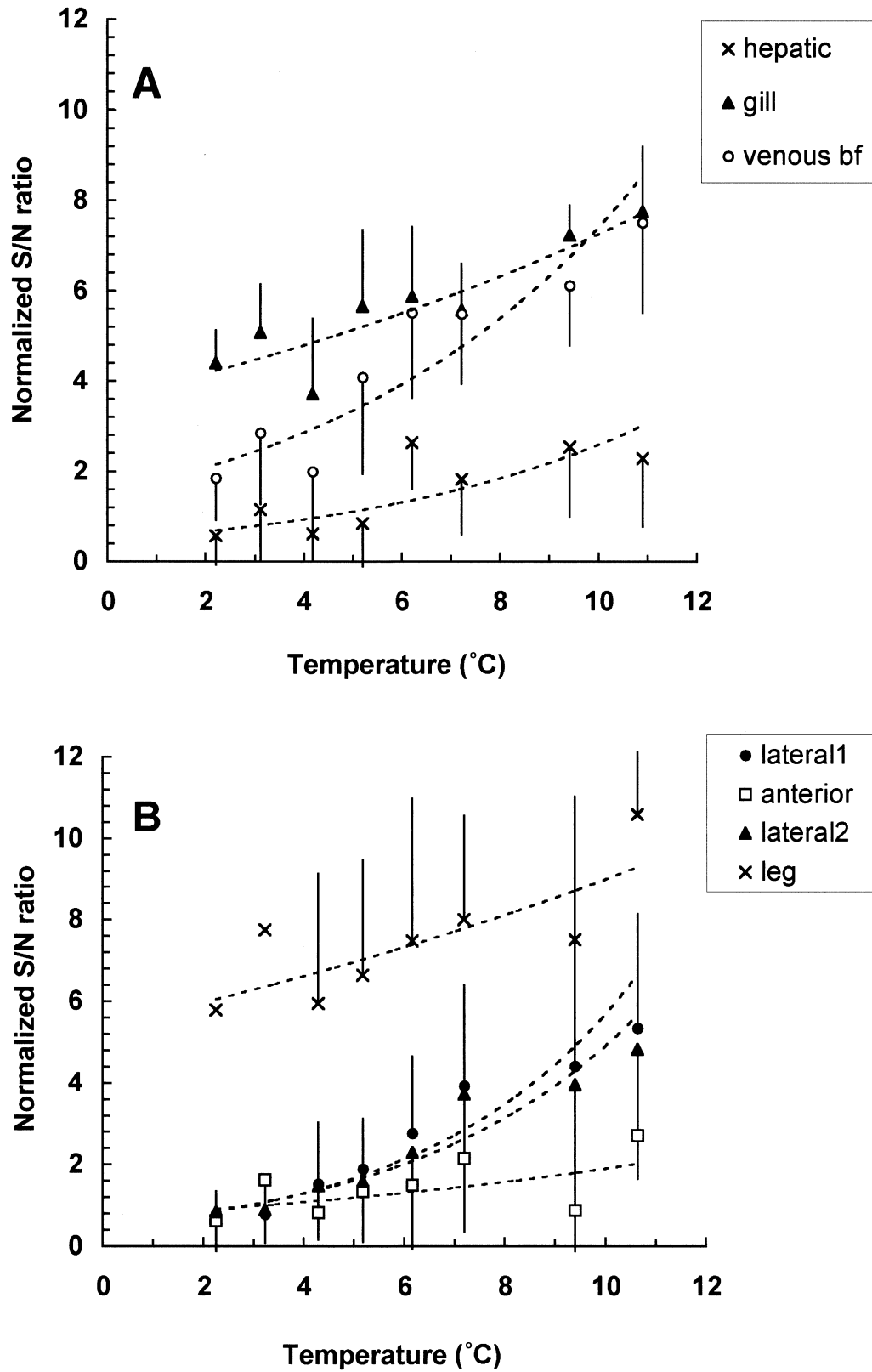
Fig. 8. Changes in haemolymph flow through different arteries given as changes in normalized S/N ratios obtained from coronal (A) and transversal (B) MR images. Flow rates decreased during cooling. Note the higher ratios for gill and leg arteries at lower temperatures in comparison to venous return, hepatic, anterior, and lateral arteries ($n = 5$ for all arteries at every temperature, except for leg artery $n = 3$, at $T = 3°C$ and $2°C$ $n = 2$).

decreased at low temperatures until low S/N ratios were reached, which correlated with the observation that flow was virtually undetectable in the MR images. Venous return decreased as well, but some flow remained visible at low temperatures (Figs. 5 arrow c, 8A), indicating the regulation of haemolymph flow by changes in the peripheral resistance of lacunes [19–21]. At all temperatures gill and leg arteries and the Aorta sternalis (Fig. 5–8) displayed a higher signal intensity than the hepatic, lateral, and anterior arteries and venous return, but the difference was small at high temperatures. In consequence, flow was maintained high through the gills and through central vessels during cooling (Fig. 5, 8), as also reflected by the Q_{10} values calculated for the different vessels. The lowest values were found for gill and leg arteries, the highest for hepatic and lateral arteries and for ventilatory flow. An intermediate Q_{10} of 6.7 was determined for venous return, which is in line with the conclusion that venous return, originates mainly from gill and central arteries in the cold (Fig. 5 arrow c). The smallest changes with temperature were observed in the anterior artery. The anterior artery displayed the lowest and most variable flow rates already under control conditions (Fig. 8 and ref. 17), therefore the S/N ratio was poor making a sensible analysis of the flow pattern impossible. Returning to control temperature reactivated ventilation and haemolymph flow within 12 h.

By including the flow measurements in the gill, leg vessels, and venous return which were not previously possible, these findings corroborate the interpretation that at low temperatures priority may be given to the maintenance of gill and locomotory function [17]. It appears from the present data (Fig. 7) that ventilation is more temperature dependent than circulation. This process can finally not be compensated for by the maintenance of haemolymph flow through the sternal and the leg arteries (Fig. 6) and oxygen deficiency results [16].

In conclusion, application of MR imaging is possible in marine crustaceans with sufficient spatial and time resolution, including investigations of individual organs over long time periods without movement artifacts. Furthermore, it is possible to monitor ventilation and blood flow simultaneously. Decreasing temperature induced a decrease in ventilatory flow as well as haemolymph flow in the marine spider crab *Maja squinado* leading to an oxygen limitation in the cold [16]. Our study supports the hypothesis that the maintenance of ventilation and circulation is critical for cold tolerance. Furthermore, haemolymph flow through some gill and leg arteries and Arteria sternalis are protected during progressive cooling emphasizing the maintenance of ventilatory and locomotory function.

Acknowledgment

References

[1] Ellington WR, Wiseman RW. Nuclear magnetic resonance spectroscopic techniques for the study of cellular functions. In: Advances in comparative and environmental physiology. Vol. 5. Berlin, Heidelberg: Springer-Verlag, 1989. p. 77–113.

[2] Van den Thillart G, van Waarde A. Nuclear magnetic resonance spectroscopy of living systems: applications in comparative physiology. Physiol Rev 1996;76:799–837.

[3] Kugel H. Improving the signal-to-noise ratio of NMR signals by reduction of inductive losses. J Magn Reson 1988;91:179–85.

[4] Doumen C, Ellington WR. Intracellular free magnesium in the muscle of osmoconforming marine invertebrate: measurement and effect of metabolic and acid-base perturbations. J Exp Zool 1992;261:394–405.

[5] Juretschke HP, Kamp G. Influence of intracellular pH on reduction of energy metabolism during hypoxia in the lugworm *Arenicola marina*. J Exp Zool 1990;256:255–63.

[6] Grøttum JA, Erikson U, Grasdalen H, Staurnes M. In vivo ^{31}P-NMR spectroscopy and respiration measurements of anaesthetized goby (*Pomatoschistus* sp.) pre-exposed to ammonia. Comp Biochem Phys A 1998;120:469–75.

[7] Pörtner HO, Bock C, Reipschlager A. Modulation of the cost of pHi regulation during metabolic depression: a 31P-NMR study in invertebrate (*Sipunculus nudus*) isolated muscle. J Exp Biol 2000;203(16): 2417–28.

[8] Blackband SJ, Stoskopf MK. In vivo nuclear magnetic resonance imaging and spectroscopy of aquatic organisms. Magn Reson Imaging 1990;8:191–8.

[9] Brouwer M, Engel DW, Bonaventura J, Johnson GA. In-vivo magnetic resonance imaging of the blue crab *Callinectes sapidus* of cadmium accumulation in tissues on proton relaxation properties. J Exp Zool 1992;263:32–40.

[10] Gardner C, Rush M, Bevilacque T. Non lethal imaging techniques for crab spermathecae. J Crust Biol 1998;18:64–9.

[11] Bock C, Sartoris FJ, Wittig RM, Pörtner HO. Temperature-dependent pH regulation in stenothermal Antarctic and eurythermal temperate eelpout (Zoarcidae): an in-vivo NMR study. Polar Biol, D01 10.1007/s003000100298.

[12] Van den Berg C, van Dusschoten D, Van As H, Terlouw A, Schaafsma TJ, Osse JWM. Visualising the water flow in a breathing carp using NMRi. Neth J of Zool 1995;45:338–46.

[13] Fernández M, Bock C, Pörtner HO. The cost of being a caring mother: the ignored factor in the reproduction of marine invertebrates. Ecol Letters 2000;3:487–94.

[14] Pörtner HO, Hardewig I, Sartoris FJ, van Dijk PLM. Energetic aspects of cold adaptation: critical temperatures in metabolic ionic and acid-base regulation? In: Pörtner HO, Playle RC, editors. Cold ocean physiology. Cambridge: University Press, 1998, p. 88–120.

[15] Pörtner HO, van Dijk PLM, Hardewig I, Sommer A. Levels of metabolic cold adaptation: tradeoffs in eurythermal and stenothermal ectotherms. In: Davidson W, Williams CH, Broady P, editors. Antartic ecosystems: models for wider ecological understanding. Christchurch, New Zealand: Caxton Press, 2000. p. 109–22.

[16] Frederich M, Pörtner HO. Oxygen limitation of thermal tolerance defined by cardiac and ventilatory performance in spider crab, *Maja squinado*. Am J Physiol 2000;279:R1531–8.

[17] Frederich M, DeWachter B, Sartoris FJ, Pörtner HO. Cold tolerance and the regulation of cardiac performance and hemolymph distribution in *Maja squinado* (Crustacea: decapoda). Physiol Biochem Zool 2000;73:406–15.

[18] Maynard DM. Circulation and heart function. In: Waterman TH, editor. The physiology of Crustacea. New York, London: Academic Press, 1960. p. 161–226.

[19] McMahon BR, Burnett LE. The crustacean open circulatory system: a reexamination. Physiol Zool 1990;63/1:35–71.

[20] Wilkens JL. Possible mechanisms of control of vascular resistance in the lobster *Homarus americanus*. J Exp Biol 1997;200:487–93.

[21] Wilkens JL, Davidson GW, Cavey MJ. Vascular peripheral resistance and compliance in the lobster *Homarus americanus*. J Exp Biol 1997;200:477–85.

[22] Haase A, Frahm J, Matthaei D, Hänicke W, Merboldt K-D. FLASH imaging. Rapid NMR imaging using low flip-angle pulses. J Magn Reson 1986;67:258–66.

[23] Hennig J, Nauerth A, Friedburg H. RARE imaging: a fast imaging method for clinical MR. Magn Reson Med 1986;3:823–33.

[24] McMahon BR, Wilkens JL. Ventilation, perfusion and oxygen uptake. In: Mantel LH, editor. The biology of crustacea. Vol. 5. New York, London: Academic Press, 1983. p. 289–372.

[25] DeWachter B, McMahon BR. Temperature effects on heart performance and regional haemolymph flow in the crab *Cancer magister*. Comp Biochem Physiol A 1996;114/1:27–33.